Mapping Longitudinal Hemispheric Structural Asymmetries of the Human Cerebral Cortex From Birth to 2 Years of Age

Gang Li[1], Jingxin Nie[1], Li Wang[1], Feng Shi[1], Amanda E. Lyall[2], Weili Lin[1], John H. Gilmore[2] and Dinggang Shen[1,3]

[1]Department of Radiology and BRIC and [2]Department of Psychiatry, University of North Carolina at Chapel Hill, NC, USA and [3]Department of Brain and Cognitive Engineering, Korea University, Seoul, Korea

Address correspondence to Dinggang Shen, Department of Radiology and BRIC, School of Medicine, University of North Carolina at Chapel Hill, MRI Building, CB #7513, 106 Mason Farm Road, Chapel Hill, NC 27599, USA. Email: dinggang_shen@med.unc.edu

Mapping cortical hemispheric asymmetries in infants would increase our understanding of the origins and developmental trajectories of hemispheric asymmetries. We analyze longitudinal cortical hemispheric asymmetries in 73 healthy subjects at birth, 1, and 2 years of age using surface-based morphometry of magnetic resonance images with a specific focus on the vertex position, sulcal depth, mean curvature, and local surface area. Prominent cortical asymmetries are found around the peri-Sylvian region and superior temporal sulcus (STS) at birth that evolve modestly from birth to 2 years of age. Sexual dimorphisms of cortical asymmetries are present at birth, with males having the larger magnitudes and sizes of the clusters of asymmetries than females that persist from birth to 2 years of age. The left supramarginal gyrus (SMG) is significantly posterior to the right SMG, and the maximum position difference increases from 10.2 mm for males (6.9 mm for females) at birth to 12.0 mm for males (8.4 mm for females) by 2 years of age. The right STS and parieto-occipital sulcus are significantly larger and deeper than those in the left hemisphere, and the left planum temporale is significantly larger and deeper than that in the right hemisphere at all 3 ages. Our results indicate that early hemispheric structural asymmetries are inherent and gender related.

Keywords: infant cortical development, infant cortical folding, infant cortical hemispheric asymmetry, longitudinal brain hemispheric asymmetry

Introduction

The adult human brain exhibits distinct hemispheric asymmetries in both structure and function. These asymmetries are thought to originate from evolutionary, developmental, hereditary, experiential, and pathological factors (Toga and Thompson 2003). A well-known example of hemispheric functional asymmetry can be seen in the specialization of the left hemisphere for language and logical processing as well as of the right hemisphere for spatial recognition (Toga and Thompson 2003; Sun and Walsh 2006). In magnetic resonance imaging (MRI) studies, cortical hemispheric structural asymmetries have been found in sulcal depth (Davatzikos and Bryan 2002; Ochiai et al. 2004; Van Essen 2005), local surface area (Lyttelton et al. 2009; Van Essen et al. 2011), cortical thickness (Luders et al. 2006; Hamilton et al. 2007; Shaw et al. 2009), gray matter density (Watkins et al. 2001; Sowell, Thompson, Peterson, et al. 2002), and vertex position (Thompson et al. 1998; Blanton et al. 2001; Sowell, Thompson, Rex, et al. 2002; Lyttelton et al. 2009). Specifically, studies in adults and children have shown prominent hemispheric asymmetries around the peri-Sylvian region and superior temporal sulcus (STS; Blanton et al. 2001; Toga and Thompson 2003; Van Essen 2005; Sun and Walsh 2006). The Sylvian fissure (SF) has been found to be longer and less sloped in the left hemisphere than in the right hemisphere (Geschwind and Levitsky 1968; Geschwind and Galaburda 1985; Thompson et al. 1998), whereas the STS has been found to be deeper and larger in the right hemisphere than in the left hemisphere (Van Essen 2005; Van Essen et al. 2011). These structural asymmetries are thought to closely relate to the functional lateralization for language processing (Toga and Thompson 2003; Dubois et al. 2010).

The existing studies of cortical hemispheric structural asymmetry have primarily focused on either adults or children, while studies in infants remain scarce (Glasel et al. 2011). Postmortem studies in infants have shown hemispheric structural asymmetries in both the STS and planum temporale (PT; Witelson and Pallie 1973; Wada et al. 1975; Chi et al. 1977). Recently, due to advances in infant brain MRI techniques and infant-specific postprocessing methods, noninvasive mapping of hemispheric structural asymmetries of the infant brain has attracted considerable attention. In utero fetal MRI studies have found curvature asymmetries in the peri-Sylvian region and STS (Habas et al. 2012) as well as a right-deeper-than-left asymmetry in the STS (Kasprian et al. 2011). Preterm newborn MRI studies have shown right-larger-than-left and right-deeper-than-left asymmetries in the STS (Dubois et al. 2008, 2010). Preterm infants have also exhibited larger posterior and anterior regions in the SF in the left hemisphere when compared with the right hemisphere (Dubois et al. 2010). Term-born infant MRI studies have identified a right-deeper-than-left asymmetry along the posterior extent of the STS and a left-deeper-than-right asymmetry centered on the PT located within the posterior SF (Hill et al. 2010). Infant MRI studies also have shown both the larger right STS and larger left PT, as well as a forward and upward shift of the posterior end of the right SF (Glasel et al. 2011). Lastly, MRI analysis of a cohort of 74 healthy neonatal subjects has demonstrated that the neonatal left hemisphere was larger than the right hemisphere (Gilmore et al. 2007). It has been suggested that these hemispheric structural asymmetries, which are clearly present in the fetal and neonatal brains, could be linked to asymmetric gene expression in the embryonic hemispheres as early as 12 gestational weeks (Sun et al. 2005).

Previous studies of hemispheric structural asymmetries in infant brains have been limited by small sample sizes, which limit the possibility of investigating sexual dimorphisms, as well as a lack of longitudinal datasets focusing on the early postnatal years. Studying the development of cortical hemispheric structural asymmetries in the early postnatal stages would increase our understanding of the origins and developmental trajectories of hemispheric asymmetries (Hill et al. 2010; Lin et al. 2012) and also provides important insights

into neurodevelopmental disorders that exhibit abnormal hemispheric asymmetries (Gilmore et al. 2007), such as autism (Chandana et al. 2005; Herbert et al. 2005; Lange et al. 2010), attention-deficit/hyperactivity disorder (Shaw et al. 2009), and schizophrenia (Sommer et al. 2001; Goldstein et al. 2002; Hamilton et al. 2007; Narr et al. 2007). To date, the longitudinal development and sexual dimorphisms of cortical hemispheric structural asymmetries in early postnatal stages still remain largely unknown. Of particular importance are the first 2 years of life, as it is considered to be the most dynamic phase of the postnatal brain development (Gilmore et al. 2007) because of the rapid changes in cortex volume, cortical surface area, and tertiary cortical folding occurring during this time (Gilmore et al. 2011; Nie, Li, et al. 2011; Li, Nie, Wang, et al. 2012). In this study, we provide the first systematic analysis of normal cortical hemispheric structural asymmetries at birth, 1, and 2 years of age using vertex position, sulcal depth, mean curvature, and local surface area, via surface-based morphometry of longitudinal MRI data from a cohort of 73 healthy subjects. Moreover, for the first time, we also investigate gender effects on the cortical hemispheric structural asymmetries at birth, 1, and 2 years of age.

Materials and Methods

Subjects

The Institutional Review Board of the University of North Carolina (UNC) School of Medicine approved this study. Pregnant mothers were recruited during the second trimester of pregnancy from the UNC hospitals. Informed consent was obtained from both parents. Exclusion criteria included abnormalities on fetal ultrasound and major medical or psychotic illness in the mother. Infants in the study cohort were free of congenital anomalies, metabolic disease, and focal lesions. Before scanning, infants were fed, swaddled, and fitted with ear protection. All infants were scanned unsedated (Gilmore et al. 2011; Shi et al. 2011).

The complete sets of longitudinal 0–1–2 year scans were acquired for 73 normal infants. The study group includes 30 singletons (20 males/10 females) and 43 twins (22 males/21 females; 7 monozygotic twin pairs, 10 dizygotic pairs, and 8 "single" twins; Gilmore et al. 2011). The mean gestational age at birth was 37.9 ± 1.6 weeks. Mean ages at the scan are: 25.5 ± 10.8, 392.8 ± 22.1, and 758.1 ± 38.1 days, respectively. For males, mean ages at the scan are: 27.3 ± 13.1, 390.0 ± 21.6, and 765.4 ± 37.4 days, respectively. For females, mean ages at the scan are: 23.0 ± 6.1, 396.6 ± 22.4, and 748.2 ± 37.4 days, respectively. There is no significant difference between males and females on all 3 scanning ages. This dataset has been used in a prior volumetric study on the development of cortical gray matter (Gilmore et al. 2011).

MRI Acquisition

Images were acquired on a Siemens head-only 3-T scanner with a circular polarized head coil. For T_1-weighted images, 160 sagittal slices were obtained by using the 3-dimensional magnetization-prepared rapid gradient-echo sequence: time repetition (TR) = 1900 ms, time echo (TE) = 4.38 ms, inversion time = 1100 ms, flip angle = 7°, and resolution = $1 \times 1 \times 1$ mm³. For T_2-weighted images, 70 transverse slices were acquired with turbo spin-echo sequences: TR = 7380 ms, TE = 119 ms, flip angle = 150°, and resolution = $1.25 \times 1.25 \times 1.95$ mm³ (Gilmore et al. 2011; Shi et al. 2011). The T_2-weighted image was linearly aligned onto the respective T_1-weighted image and further resampled to be $1 \times 1 \times 1$ mm³. Data were collected longitudinally at 3 age groups: Neonates (0-year old or birth), 1-year old, and 2-year old. Data with motion artifacts were discarded, and a rescan was made when possible.

Image Processing and Surface Mapping

All MRIs were processed using the following procedures: 1) Skull stripping (Shi et al. 2012), followed by a manual review to ensure the accurate removal of nonbrain tissues, 2) the removal of the cerebellum and brain stem using in-house developed registration toolkits (Wu et al. 2006), 3) the correction of intensity inhomogeneity using N3 (Sled et al. 1998), 4) the rigid alignment of all images at each age to the age-matched infant brain MRI atlas (Shi et al. 2011). Tissue segmentation of infant brain MRIs was performed by a infant-specific longitudinally guided coupled level sets method (Wang et al. 2011), which combines local intensity information, spatial prior information, cortical thickness constraints, and longitudinal information by longitudinal image registration (Shen and Davatzikos 2004; Xue et al. 2006; Shi et al. 2010) into a variational framework. After tissue segmentation, noncortical structures were masked and filled, and each brain was further separated into the left and right hemispheres. Supplementary Figure S1a,b show examples of T_2-weighted MRIs at birth and their corresponding tissue segmentation results, respectively.

Based on tissue segmentation results, topologically correct and geometrically accurate cortical surfaces of each hemisphere for each image were reconstructed by using a deformable surface method (Li, Nie, Wu, et al. 2012). Specifically, the white matter of each hemisphere was first topologically corrected to ensure a spherical topology, and then the corrected white matter was tessellated to form a triangulated surface mesh. Finally, the triangulated surface mesh of each hemisphere was deformed toward the reconstruction of the inner, central, and outer cortical surfaces by preserving its initial topology. The central cortical surface, which was defined as the layer lying in the geometric center of the cortex, was adopted for analyzing hemispheric asymmetries, since it provides a more balanced representation of gyral and sulcal regions (Van Essen 2005; Van Essen and Dierker 2007; Lyttelton et al. 2009). Supplementary Figure S1c,d show examples of reconstructed inner and central cortical surfaces, respectively. Supplementary Figure S2 shows examples of reconstructed cortical surfaces embedded in the several axial slices of the T_2-weighted MRI of a subject at birth. The cortical surfaces of the right hemisphere were mirror-flipped to the corresponding left hemisphere along the midsagittal plane in order to perform hemispheric asymmetry analysis (Lyttelton et al. 2009). All inner cortical surfaces, which had vertex-to-vertex correspondences with the central cortical surfaces, were smoothed, inflated, and mapped to standard spheres by minimizing the metric distortion between the cortical surface and its spherical representation for performing cortical surface alignment (Fischl et al. 1999).

The hemisphere-unbiased surface-based atlas of cortical structures at each age was first constructed by groupwise registration of the left and mirror-flipped right cortical surfaces of all subjects by using Spherical Demons (Yeo et al. 2010). The generated atlases captured the variability of cortical folding and ensured that there was no bias for any particular individual and hemisphere. Then, the left and mirror-flipped right cortical surfaces of all subjects at each age were aligned to the age-matched hemisphere-unbiased surface-based atlas. Supplementary Figure S1e,f show examples of spherical representations of the left and mirror-flipped right cortical surfaces and their corresponding aligned spherical representations, respectively. At each age, the left and mirror-flipped right central cortical surfaces of each subject were resampled based on the deformation from the hemisphere-unbiased surface-based atlas to the individual cortical surfaces to standard-mesh tessellations with 163 842 vertices. This step establishes the vertex-to-vertex correspondences across all subjects and hemispheres at the same age. The local surface area of each vertex on the central cortical surface was computed as one-third the sum of the areas of all triangles associated with that vertex (Lyttelton et al. 2009). Sulcal depth, which provided a continuously varying measure of both coarse and fine cortical shape attributes (Van Essen 2005), was computed on each vertex on the central cortical surface. Specifically, cerebral hull volume, defined by a boundary running along the margins of gyri without dipping into sulci, was first generated by carving the central cortical surface as a closed volume followed by 6 iterations of dilation and 6 iterations of erosion (Van Essen 2005). The sulcal depth was defined as the distance from each

vertex on the central cortical surface to the nearest point in the cerebral hull surface (Van Essen 2005; Hill et al. 2010). Supplementary Figure S3 shows sulcal depth maps on the central cortical surfaces of the left hemispheres of a representative subject at birth, 1, and 2 years of age. Supplementary Figure S4 shows average sulcal depth maps of the left hemispheres of all subjects at birth, 1, and 2 years of age on the age-matched inflated cortical surfaces. Mean curvature, which provided an intuitive indication of local cortical folding of gyri and sulci (Cachia et al. 2003; Dubois et al. 2008; Nie et al. 2010; Habas et al. 2012), was also computed on each vertex on the central cortical surface. Herein, we adopt the outward oriented normal direction field for a close comparison with some existing studies (Cachia et al. 2003; Dubois et al. 2008; Habas et al. 2012). The mean curvatures on the gyral crests and sulcal bottoms are positive and negative values (Li et al. 2010), respectively. Supplementary Figure S5 shows the mean curvature maps on the central cortical surfaces of the left hemisphere of a representative subject at birth, 1, and 2 years of age. Supplementary Figure S6 shows average mean curvature maps of the left hemispheres of all subjects at birth, 1, and 2 years of age on the age-matched inflated cortical surfaces.

Testing Significance of Hemispheric Asymmetries

To test the significance of left–right hemispheric asymmetries of the sulcal depth, mean curvature, and local surface area, we utilized the surface-based threshold-free cluster enhancement (TFCE) method (Hill et al. 2010), previously used in infants and adults for testing the significance of hemispheric asymmetries of the sulcal depth (Hill et al. 2010) and local surface area (Van Essen et al. 2011). First, the left and right hemispheres of each subject at each age were paired together. Next, we calculated a paired t-statistic on each cortical attribute at each surface vertex, such as sulcal depth, mean curvature, and local surface area with no spatial smoothing. Thirdly, the sign of subjects' sulcal depth, mean curvature, and local surface area was randomly flipped 2500 times, and the corresponding paired t-maps were generated (Hill et al. 2010). Fourthly, each t-map was smoothed at 0.5 strength with 9 iterations using an average neighbor algorithm (Hill et al. 2010). Finally, TFCE, a method originally developed for the volumetric data (Smith and Nichols 2009), was used to identify statistically significant clusters (Hill et al. 2010).

To test the significance of left–right hemispheric asymmetries of the 3-dimensional (3D) vertex positions, we utilized SurfStat (Chung et al. 2010), a toolbox for the statistical analysis of multivariate surface data based on random field theory (Worsley et al. 2004) that has been used for the mapping of hemispheric asymmetries of vertex positions in adults (Lyttelton et al. 2009). Multivariate random field theory is built based on modeling the Hotelling's T as a smooth random field and provides a suitable approximation for the distribution of its maximum T_{max} (Lyttelton et al. 2009). Random field theory generates a decision threshold t_α that has been corrected for multiple comparisons, such that the probability of T_{max} exceeding t_α is less or equal to $\alpha = 0.05$, and significant regions are detected as regions with T exceeding t_α (Cao and Worsley 1999).

Results

Vertex Position Asymmetries at Birth, 1, and 2 Years of Age

The first, second, and third rows in Figure 1 show the vertex position asymmetries between left and mirror-flipped right hemispheres at birth, 1, and 2 years of age for both lateral and medial views for the whole population, males, and females, respectively. On the lateral surface, Figure 1a,b shows the average cortical surfaces of left and mirror-flipped right hemispheres color-coded by the magnitude of the deformation field between their respective average cortical surfaces. Similarly, on the medial surface, Figure 1d,e shows the average cortical surfaces of left and mirror-flipped right

hemispheres color-coded by the magnitude of the deformation field between their respective average cortical surfaces. After affine alignment to the age-matched infant brain image atlas (Shi et al. 2011), the average cortical surface of each hemisphere for each age was generated by averaging the 3D positions of corresponding vertices of all cortical surfaces of the hemisphere. The major cortical folding patterns are strikingly similar between left and right hemispheres. Figure 1c,f shows clusters that passed significance testing of 3D vertex position asymmetry. The arrows in Figure 1c,f indicate the deformation field from the average cortical surface of the left hemispheres to the average cortical surface of the mirror-flipped right hemispheres.

On the lateral surface, the temporal lobe, inferior parietal cortex, and SF are consistently identified as regions with significant asymmetries at birth, 1, and 2 years of age. Males have consistently larger sizes of significant clusters than females at birth, 1, and 2 years of age. The temporal pole only exhibits significance at birth, but not at 1 and 2 years of age. Prominent asymmetries are consistently observed around the supramarginal gyrus (SMG) at birth, 1, and 2 years of age. Males also consistently have larger magnitudes of asymmetries than females at birth, 1, and 2 years of age. The left SMG is found to be located up to 10.2 mm posterior for males (6.9 mm for females) when compared with the right SMG at birth. This difference increases to up to 12.0 mm for males (8.4 mm for females) by 2 years of age. Another subtle, but significant, asymmetry consistently observed is near the ventral tip of the postcentral gyrus at birth, 1, and 2 years of age for both males and females. The left hemisphere has a more pronounced gyral bulge than the right hemisphere.

On the medial surface, the parieto-occipital sulcus, a portion of the medial orbital frontal cortex, and the posterior cingulate cortex are consistently identified as regions with significant asymmetries at birth, 1, and 2 years of age. Prominent asymmetries are consistently observed around the cuneus cortex. A greater number of regions show significance at birth, but these regions eventually shrink to smaller regions or disappear at 1 and 2 years of age. Males consistently exhibit larger sizes of significant clusters and magnitudes of asymmetries than females at birth, 1, and 2 years of age. In general, gender-related prominent hemispheric vertex position asymmetries are established at birth and continue to evolve modestly from birth to 2 years of age, with the overall patterns of shrinking significant regions and increasing the magnitudes of asymmetries.

Sulcal Depth Asymmetries at Birth, 1, and 2 Years of Age

The first, second, and third rows in Figure 2 show the sulcal depth asymmetries between the left and right hemispheres at birth, 1, and 2 years of age for both the lateral and medial views for the whole population, males, and females, respectively. All results are shown on the age-matched inflated average cortical surface of left hemispheres. Figure 2a,d shows the differences between sulcal depth maps of the left and right hemispheres. On the lateral surface, the patterns of left-deeper-than-right (red color) and right-deeper-than-left (blue color) are qualitatively similar at birth, 1, and 2 years of age. The magnitude of left–right sulcal depth difference steadily increases from birth to 2 years of age, consistent with the pattern of sulcal depth increasing from birth to 2 years of age
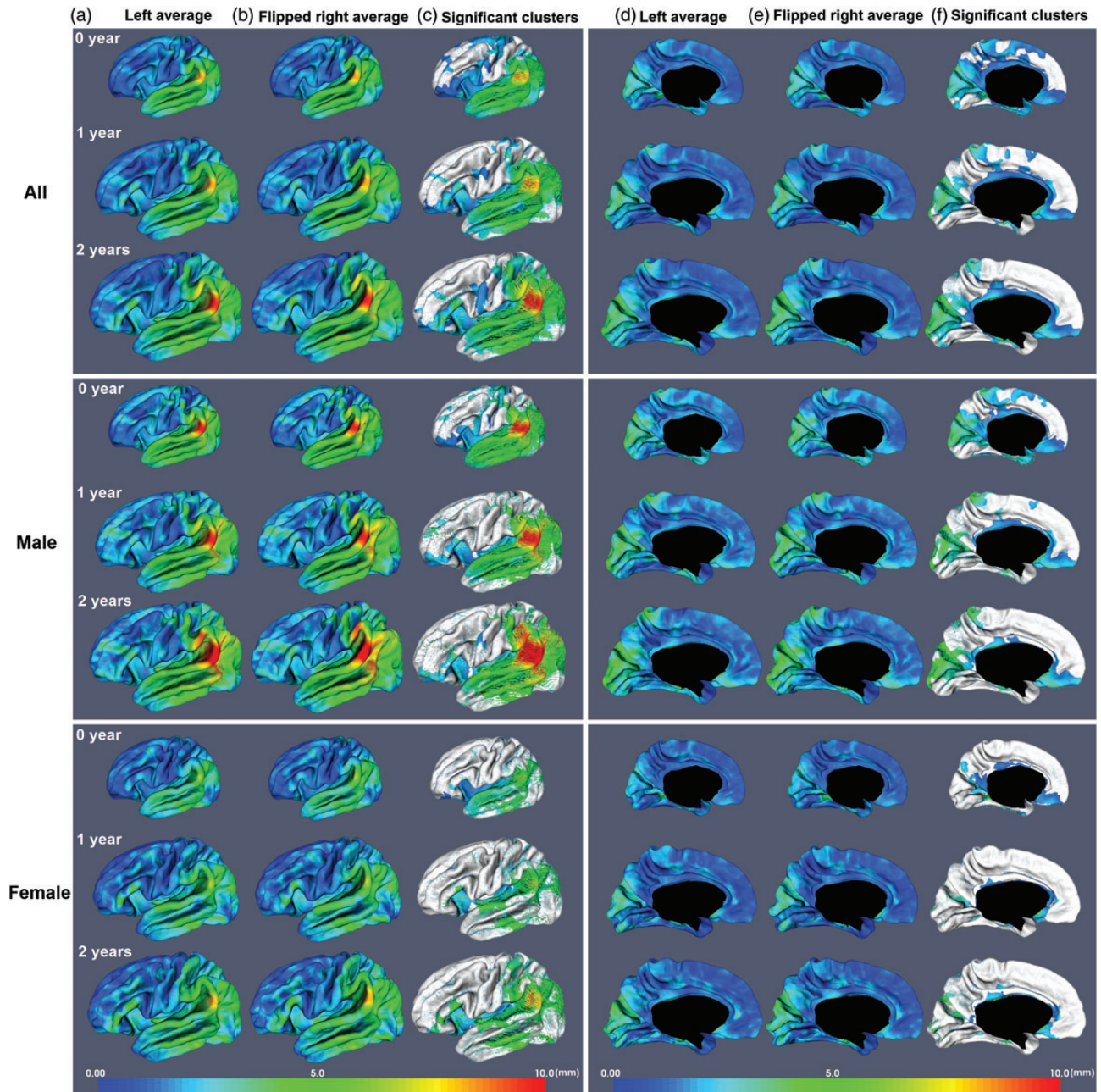
Figure 1. Hemispheric vertex position asymmetries of the cortex. (*a*) and (*d*) Average cortical surface of left hemispheres. (*b*) and (*e*) Average cortical surface of mirror-flipped right hemispheres. (*c*) and (*f*) Significant clusters (nonwhite colors) of vertex position asymmetries shown on the left average cortical surface. (*a*), (*b*), (*d*), and (*e*) are color-coded by the magnitude of deformation field from the average surface of left hemispheres to the average surface of mirror-flipped right hemispheres as shown by color arrows in (*c*) and (*f*). *a–c* show the lateral view, and *d–f* show the medial view.

as shown in Supplementary Figure S4. Males have consistently larger differences of left–right sulcal depth than females at birth, 1, and 2 years of age. On the medial surface, the patterns of left-deeper-than-right (red color) and right-deeper-than-left (blue color) are also qualitatively similar at birth, 1, and 2 years of age; however, the magnitude of left–right sulcal depth difference is not very consistent from birth to 2 years of age. Figure 2*b,e* shows the *t*-statistic maps, and Figure 2*c,f* shows clusters that passed significance testing (*P* < 0.01) by the TFCE method.

On the lateral surface, 4 significant clusters are consistently identified at birth, 1, and 2 years of age in the whole population. These clusters include a left-deeper-than-right asymmetry at the peri-Sylvian region around the PT, a right-deeper-than-left asymmetry along the middle extent of the STS, a right-deeper-than-left asymmetry in a portion of the SMG, and a right-deeper-than-left asymmetry at the dorsolateral part of the central sulcus. Table 1 provides the mean and standard deviation of the left–right differences of average sulcal depth for the 4 clusters of asymmetries in all subjects at birth, 1, and 2 years of age. Considerable gender effects on the cortical hemispheric sulcal depth asymmetry are found at birth, 1, and 2 years of age. In males, 3 clusters of the above 4 significant clusters are consistently identified at birth, 1, and 2
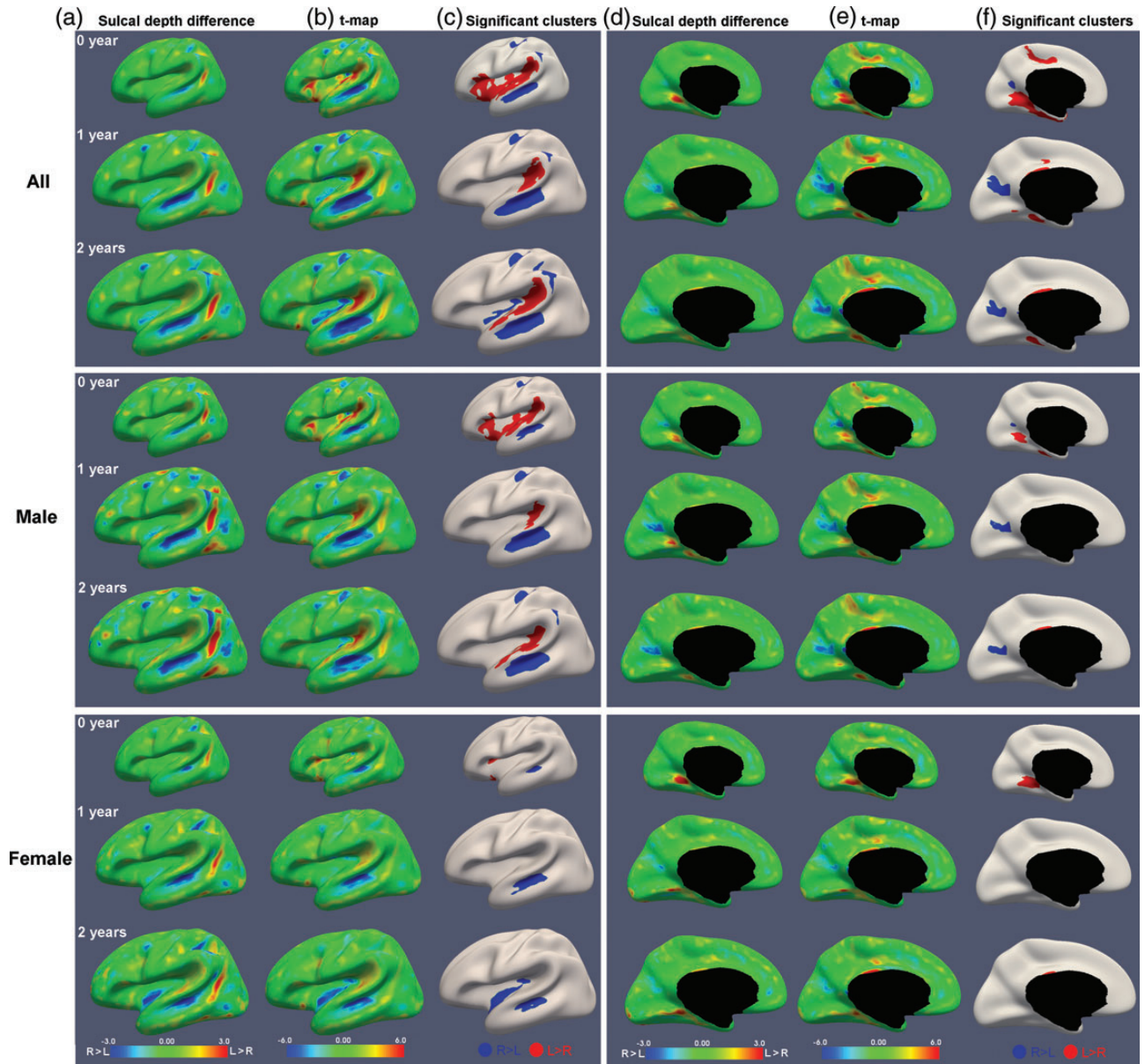
Figure 2. Hemispheric sulcal depth asymmetries of the cortex. (a) and (d) Maps of average sulcal depth difference between the left and right hemispheres. (b) and (e) Paired t-statistic map of hemispheric sulcal depth difference. (c) and (f) Significant clusters of sulcal depth asymmetries by the TFCE method ($P < 0.01$). Blue clusters are deeper on the right than on the left, and red clusters are deeper on the left than on the right. a–c show the lateral view, and d–f show the medial view.

Table 1
The left–right mean sulcal depth differences of significant clusters at birth, 1, and 2 years of age

Left–right sulcal depth differences of significant clusters	0 year (mm)		1 year (mm)		2 years (mm)	
	Males	Females	Males	Females	Males	Females
Superior temporal sulcus	−1.23 ± 1.21	−1.15 ± 1.09	−1.94 ± 1.45	−1.51 ± 1.34	−1.92 ± 1.58	−1.52 ± 1.40
Dorsolateral central sulcus	−1.00 ± 1.02	−0.77 ± 1.47	−1.43 ± 1.66	−0.73 ± 1.8	−1.34 ± 1.57	−0.80 ± 1.65
Supramarginal gyrus	−1.40 ± 2.02	−1.07 ± 2.09	−1.74 ± 3.04	−1.57 ± 2.93	−1.80 ± 2.77	−1.87 ± 2.65
Sylvian fissure	0.57 ± 0.38	0.40 ± 0.42	0.95 ± 1.19	0.79 ± 0.93	1.04 ± 1.05	0.90 ± 1.08
Parieto-occipital sulcus	−1.27 ± 1.64	−0.81 ± 1.9	−1.54 ± 1.95	−1.03 ± 1.82	−1.52 ± 1.99	−0.99 ± 1.72

years of age, except the right-deeper-than-left asymmetry in the SMG which is only shown at 2 years of age. In females, only the cluster of right-deeper-than-left asymmetry in the STS is consistently shown at birth, 1, and 2 years of age. The right STS is up to 2.1 mm deeper in males (2.8 mm for females) than the left STS at birth, a difference that increases up to 3.3 mm for males (3.8 mm for females) by 2 years of age. As shown in Table 1, males consistently have larger mean left–right sulcal depth in STS than females at birth, 1, and 2 years of age. The location of maximum left–right sulcal

depth asymmetry in the STS of males is more anterior than that of females. Males consistently have a larger cluster of left–right sulcal depth asymmetry in STS than females at birth, 1, and 2 years of age. In females, although the peri-Sylvian region around PT does not show significant asymmetry with $P < 0.01$, this region is consistently identified as significance with $P < 0.05$ at birth, 1, and 2 years of age as shown in Supplementary Figure S7. Interestingly, in both males and females, left-deeper-than-right asymmetry appears at the anterior portion of the SF at birth, but disappears at 1 and 2 years of age. Moreover, the middle portion of the SF shows a left-deeper-than-right asymmetry at birth in males, nonsignificant asymmetry at 1 year of age in both males and females, and a right-deeper-than-left asymmetry at 2 years of age in females.

On the medial surface, 2 significant clusters are consistently identified at birth, 1, and 2 years of age in the whole population, including a left-deeper-than-right asymmetry in the parahippocampal region and a right-deeper-than-left asymmetry in the parieto-occipital sulcus. At birth, the cluster of right-deeper-than-left asymmetry in the parieto-occipital sulcus is relatively small; however, this cluster increases to relatively larger cluster at 1 and 2 years of age. The cluster of left-deeper-than-right asymmetry in the parahippocampal region is large at birth, yet gradually shrinks to a small cluster from birth to 2 years of age. Similarly, a left-deeper-than-right asymmetry in the posterior cingulate sulcus is shown at birth, but also shrinks to a smaller cluster at 1 year of age, and eventually disappears at 2 years of age, despite the t-statistic maps being similar to each other at all 3 time points. In males, the cluster of right-deeper-than-left asymmetry in the parieto-occipital sulcus is consistently shown at birth, 1, and 2 years of age, whereas the cluster of left-deeper-than-right asymmetry in the parahippocampal region is only shown at birth. In males, the right parieto-occipital sulcus is up to 1.9 mm deeper than the left parieto-occipital sulcus at birth, a difference that increases to up to 2.4 mm by 2 years of age. In females, no asymmetry has been found in parieto-occipital sulcus at birth, 1, and 2 years of age, and the cluster of left-deeper-than-right asymmetry in the parahippocampal region is only shown at birth. In general, gender-related hemispheric sulcal depth asymmetries are present at birth and continue to evolve modestly from birth to 2 years of age.

Mean Curvature Asymmetries at Birth, 1, and 2 Years of Age

The first, second, and third rows in Figure 3 show the mean curvature asymmetries between the left and right hemispheres at birth, 1, and 2 years of age for both lateral and medial views for the whole population, males, and females, respectively. All results are shown on the age-matched inflated average cortical surface of left hemispheres. Figure 3a,c shows the differences between mean curvatures of the left and right hemispheres. Figure 3b,e shows the t-statistic maps, and Figure 3c,f shows clusters that pass significance testing ($P < 0.01$) by the TFCE method.

On the lateral surface, a right-larger-than-left mean curvature asymmetry in the posterior temporal operculum is shown at birth, but shrinks to a smaller cluster at 1 year of age, and eventually disappears by 2 years of age. The left–right mean curvature asymmetry difference in this region at birth and 1

year of age can reach up to 0.15. A left-larger-than-right mean curvature asymmetry in the Heschl's gyrus is present at 1 year of age, but not at birth or 2 years of age. In males, only the cluster of right-larger-than-left mean curvature asymmetry in the posterior temporal operculum is shown at birth. In females, the small cluster of left-larger-than-right mean curvature asymmetry in the Heschl's gyrus is present at 1 year of age, and a small cluster of right-larger-than-left mean curvature asymmetries are present in the middle portion of the SF at 2 years of age.

On the medial surface, a cluster of right-larger-than-left mean curvature asymmetry, with a left–right difference up to 0.15, is shown at birth in the whole population, but not at 1 or 2 years of age. In males, only a right-larger-than-left mean curvature asymmetry is shown in the medial orbital frontal cortex at birth. In females, a cluster of right-larger-than-left mean curvature asymmetry and several small clusters of left-larger-than-right mean curvature asymmetries around the parahippocampal region are shown at birth. No cluster of asymmetry has been found at 1 and 2 years of age for both males and females. Overall, hemispheric mean curvature asymmetries are gender-related and evolve from birth to 2 years of age.

Local Surface Area Asymmetries at Birth, 1, and 2 Years of Age

The first, second, and third rows in Figure 4 show the local surface area asymmetries between the left and right hemispheres at birth, 1, and 2 years of age for both lateral and medial views for the whole population, males, and females, respectively. All results are shown on the age-matched inflated average cortical surface of left hemispheres. Figure 4a,d shows the ratio of mean vertex area between the left and right hemispheres. On the lateral and medial surfaces, the patterns of left-larger-than-right (red color) and right-larger-than-left (blue color) are qualitatively similar at birth, 1, and 2 years of age. Leftward asymmetries are most prominent in the SF, and rightward asymmetries are most prominent in the inferior parietal cortex and the posterior portion of the STS. Figure 4b,e shows the t-statistic maps, and Figure 4c,f shows clusters that passed significance testing ($P < 0.01$) by the TFCE method.

On the lateral surface, several significant clusters of asymmetries are consistently identified at birth, 1, and 2 years of age in the whole population, including leftward asymmetries in the anterior and posterior portions of the SF, postcentral sulcus, and temporal pole, as well as rightward asymmetries in the STS and inferior parietal cortex. A large portion of the middle frontal, precentral, and postcentral gyri show leftward asymmetries at birth, yet these asymmetric clusters disappear at 1 and 2 years of age. Table 2 shows the left–right area differences of significant clusters at birth, 1, and 2 years of age. In males, leftward asymmetries show similar patterns to those of the whole population. Rightward asymmetries in males are mainly located in the inferior parietal cortex at birth, 1, and 2 years of age. In females, leftward asymmetries are mainly located in the anterior and posterior portions of the SF, whereas rightward asymmetries are primarily located in the STS at birth, 1, and 2 years of age. In addition, females also show leftward asymmetries in the posterior portion of the postcentral gyrus and rightward asymmetries in a portion of the inferior parietal cortex at 2 years of age.
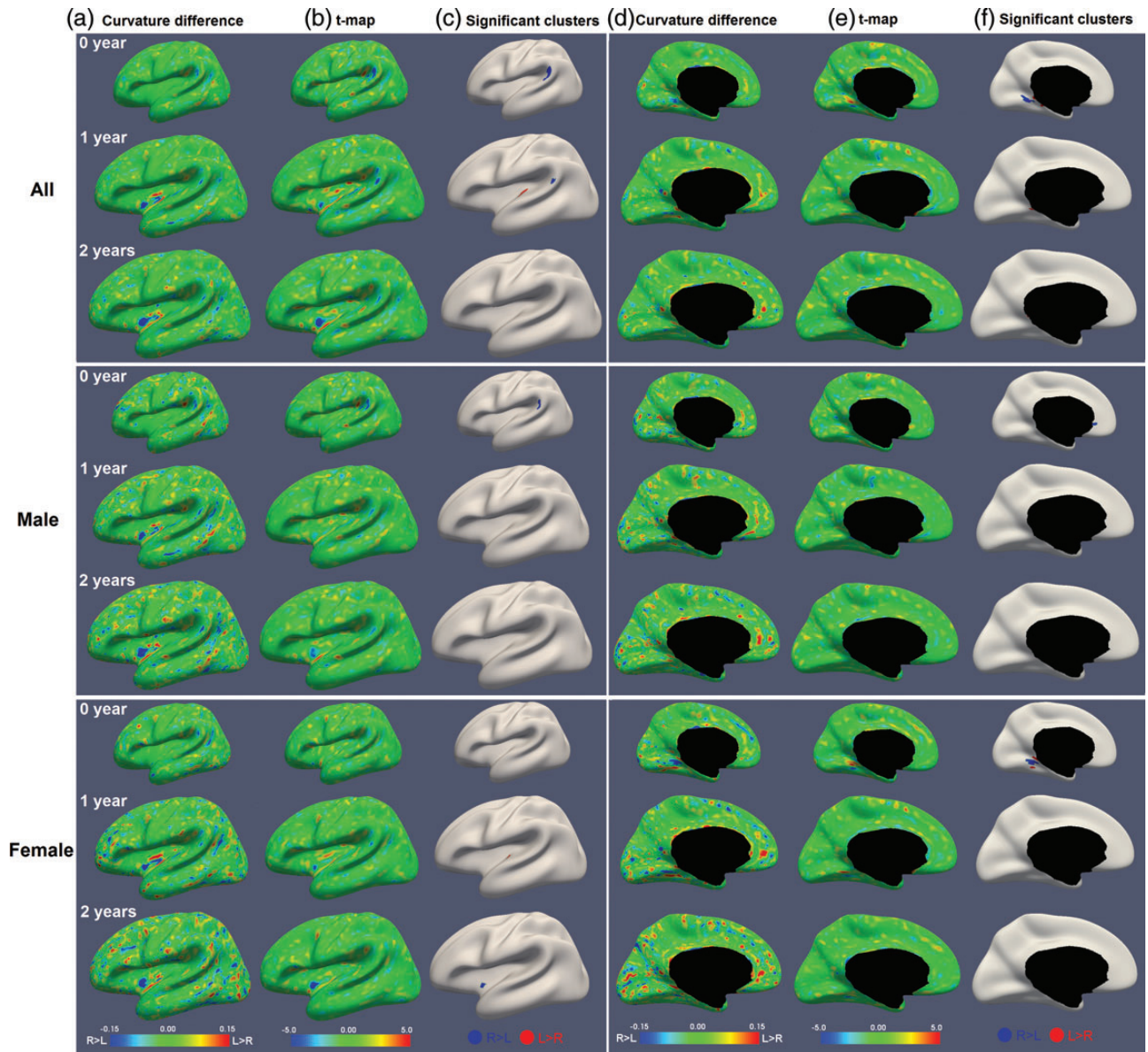
Figure 3. Hemispheric mean curvature asymmetries of the cortex. (a) and (d) Maps of average mean curvature difference between the left and right hemispheres. (b) and (e) Paired *t*-statistic map of hemispheric mean curvature difference. (c) and (f) Significant clusters of mean curvature asymmetries by the TFCE method (*P* < 0.01). Blue clusters are larger on the right than on the left, and red clusters are larger on the left than on the right. *a–c* show the lateral view, and *d–f* show the medial view.

On the medial surface, leftward asymmetries are found in the paracentral lobule, posterior cingulate, fusiform cortices, and a portion of both the medial superior frontal and the medial orbital frontal cortices at birth. However, leftward asymmetries are found only in small regions of the paracentral lobule and posterior cingulate cortex at 1 and 2 years of age, although the *t*-statistic maps seem similar to each other at all 3 time points. A small cluster of rightward asymmetry in the parieto-occipital sulcus is found at birth, and this cluster expands to contain a large portion of the parieto-occipital sulcus and cuneus cortex at 1 and 2 years of age. In males, leftward asymmetries are found in the paracentral lobule, posterior cingulated cortex, and calcarine sulcus at birth. Rightward asymmetries are found in males in the parieto-occipital sulcus and cuneus cortex at 1 and 2 years of age. In females, a small cluster of rightward asymmetry is found in the isthmus cortex at 1 year of age, and a small cluster of leftward

asymmetry is found in the paracentral lobule at 2 years of age. Overall, gender-related hemispheric local surface area asymmetries emerge at birth and exhibit differential patterns of development from birth to 2 years of age.

Discussion

Cortical hemispheric structural asymmetries are present at birth, suggesting that cortical asymmetries arise in the fetus and continue evolve from birth to 2 years of age. Prominent cortical structural asymmetries are found around the peri-Sylvian regions that are related to speech perception and production in the adult brain (Dehaene-Lambertz et al. 2006). Considerable gender effects on cortical structural asymmetries exist at birth, which indicate that sexual dimorphisms arise before birth and persist from birth to 2 years of age, with males consistently having larger sizes of significant clusters
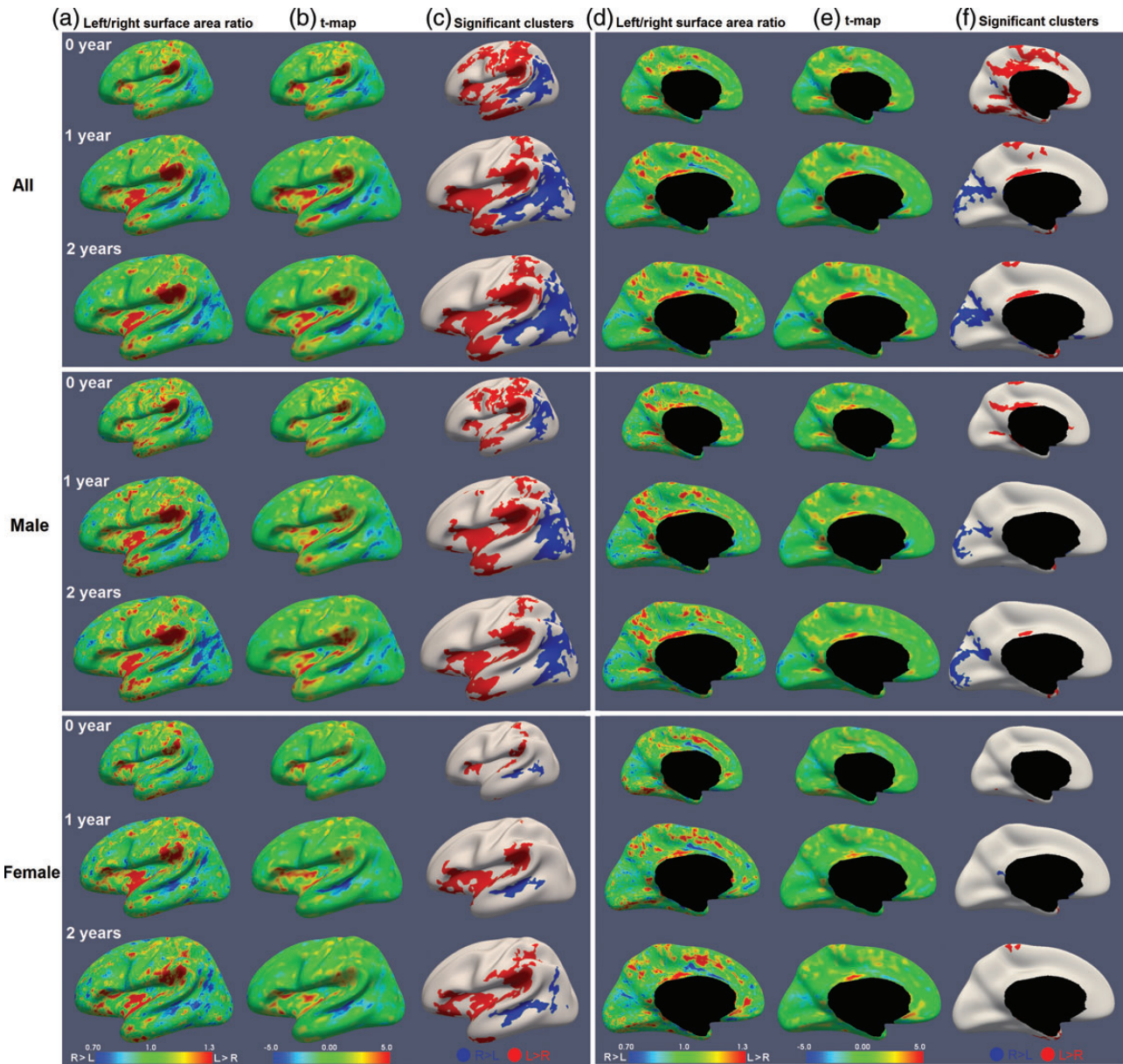
Figure 4. Hemispheric local surface area asymmetries of the cortex. (a) and (d) Maps of the ratio of average local surface area between the left and right hemispheres. (b) and (e) Paired *t*-statistic map of hemispheric local surface area difference. (c) and (f) Significant clusters of local surface area asymmetries by the TFCE method (*P* < 0.01). Blue clusters are larger on the right than on the left, and red clusters are larger on the left than on the right. *a–c* show the lateral view, and *d–f* show the medial view.

Table 2
The left–right area differences of significant clusters at birth, 1, and 2 years of age

Left–right area differences of significant clusters	0 year (mm^2)		1 year (mm^2)		2 years (mm^2)	
	Males	Females	Males	Females	Males	Females
Left > right clusters	1366 ± 394	1095 ± 351	1462 ± 539	1355 ± 445	1768 ± 623	1511 ± 488
Right > left clusters	−404 ± 246	−297 ± 209	−1380 ± 572	−1012 ± 547	−1736 ± 638	−1394 ± 653

and magnitudes of asymmetries than females at birth, 1, and 2 years of age.

On the lateral surface, prominent vertex position asymmetries were consistently observed around the SMG, with the left SMG being significantly posterior to the right SMG, consistent with the previous studies in infants (Glasel et al. 2011), and the magnitude of the asymmetries increasing from birth to 2 years of age. Previous studies have shown significant position asymmetry around the peri-Sylvian region and SMG in adults and children (Thompson et al. 1998; Blanton et al. 2001; Narr, Thompson, Sharma, Moussai, Zoumalan, et al. 2001; Sowell, Thompson, Rex, et al. 2002; Toga and Thompson 2003; Lyttelton et al. 2009; Van Essen et al. 2011). We also found that males have larger magnitudes of vertex position

asymmetries around the SMG than females at birth, 1, and 2 years of age. Although males have larger brain volumes than females, this factor should not have affected our reported vertex position asymmetries as the magnitudes of vertex position asymmetries were computed on the cortical surfaces affine-normalized with the atlas (Shi et al. 2011) in order to remove the size effect. This result is generally consistent with the report that the slope of the STS in the right hemisphere is significantly steeper in males than in females in adults (Narr, Thompson, Sharma, Moussai, Blanton, et al. 2001). On the medial surface, prominent asymmetries were consistently observed around the cuneus cortex at birth, 1, and 2 years of age, largely reflecting the occipital petalia, where the left occipital pole was displaced toward the right occipital pole (Toga and Thompson 2003), consistent with the findings in adults (Lyttelton et al. 2009; Van Essen et al. 2011). A greater number of regions show significance at birth, but these regions shrink at 1 and 2 years of age, suggesting the modest evolution of cortical hemispheric asymmetries of vertex positions from birth to 2 years of age. Males consistently have larger magnitudes and sizes of the significant clusters of vertex position asymmetries than females at birth, 1, and 2 years of age, suggesting that sexual dimorphisms arise before birth and persist from birth to 2 years of age. Of note, previous reports have indicated a greater degree of functional asymmetry in males than in females in adults (McGlone 1978; Shaywitz et al. 1995; Draca 2010).

On the lateral surface, we found a left-deeper-than-right asymmetry around the PT of the posterior SF consistently at birth, 1, and 2 years of age, in agreement with the existing studies on sulcal depth asymmetries in term-born infants (Hill et al. 2010) and adults (Van Essen 2005). We also found a right-deeper-than-left asymmetry along the middle extent of STS consistently at birth, 1, and 2 years of age, similar to the findings in the existing studies on sulcal depth asymmetries in fetuses (Kasprian et al. 2011), premature newborns (Dubois et al. 2008), term infants (Hill et al. 2010; Glasel et al. 2011), and adults (Van Essen 2005). To better illustrate the right-deeper-than-left asymmetry in the STS, Supplementary Figure S8 shows a cutting view of overlap of the left average cortical surface and the mirror-flipped right average cortical surface around the STS at birth, where one can clearly see that the right STS is deeper and larger than the left STS. This asymmetry may be explained by the fact that the STS appears 1 or 2 weeks earlier on the right hemisphere than on the left hemisphere in fetuses (Chi and Dooling 1976; Kasprian et al. 2011; Habas et al. 2012). Therefore, the left-deeper-than-right asymmetry around the PT and the right-deeper-than-left asymmetry in the STS seem to be intrinsic hemispheric sulcal depth asymmetries across the lifespan. However, this finding needs to be confirmed with the studies of developmental trajectories of asymmetries of the sulcal depth in childhood and adolescence. Moreover, males consistently have more prominent asymmetries of sulcal depth around the PT and STS than females at birth, 1, and 2 years of age, suggesting that the gender effects on sulcal depth asymmetries arise before birth and persist from birth to 2 years of age. Furthermore, we found that the right posterior temporal operculum was more convex than the left posterior temporal operculum at birth and 1 year of age, consistent with the recent findings in the fetus after 23 gestational weeks (Habas et al. 2012). On the medial surface, we identified a right-deeper-than-left

asymmetry at the parieto-occipital sulcus consistently at birth, 1, and 2 years of age in males, but not in females. Previous studies have shown the same significant right-deeper-than-left asymmetry in the adults (Hill et al. 2010). At birth, the cluster of left-deeper-than-right asymmetry around the parahippocampal cortex was large, but then subsequently shrunk to a small region at 1 and 2 years of age. Moreover, a cluster of right-larger-than-left and 2 small clusters of left-larger-than-right asymmetries of mean curvatures near the parahippocampal cortex were shown at birth in females, but not at 1 or 2 years of age in neither males nor females. This result might relate to the findings of greater convexity of the right parahippocampal cortex than the left parahippocampal cortex in fetal brains (Habas et al. 2012). These patterns might reflect the gender-related evolution of cortical asymmetries of sulcal depth and mean curvature from birth to 2 years of age.

Leftward local surface area asymmetries were consistently found at the anterior and posterior portions of the SF, postcentral sulcus, and temporal pole, whereas rightward asymmetries were consistently found at the STS, inferior parietal cortex, cuneus cortex, and parieto-occipital sulcus at birth, 1, and 2 years of age, consistent with the reports of a larger left PT and a larger right STS in infants (Glasel et al. 2011). In adults, similar local surface area asymmetry patterns have been reported in the parietal, temporal, and occipital lobes (Van Essen et al. 2011). In our study, we found one instance of leftward asymmetry in the middle frontal gyrus at birth in males, but not in females. Our results were also generally consistent with the results in adults in Lyttelton et al. (2009), which showed leftward asymmetries in the SMG, superior temporal plane, and anterior portion of the superior temporal gyrus, as well as rightward asymmetries in the anterior occipital lobes. At birth, regions with leftward area asymmetry were much larger than that with rightward area asymmetry, consistent with the report of the volume and surface area of the left hemisphere being significantly larger than that of the right hemisphere in neonatal brains (Gilmore et al. 2007; Li, Nie, Wang, et al. 2012). From birth to 2 years of age, regions with leftward asymmetry decreased and regions with rightward asymmetry increased, consistent with the report of similar left and right surface areas at 1 and 2 years of age (Li, Nie, Wang, et al. 2012).

The largest leftward area asymmetry was consistently found in the posterior part of area OP1 (the most caudal area of the parietal operculum) at birth, 1, and 2 years of age, consistent with the area asymmetry study in adults (Van Essen et al. 2011) and reported findings of significantly larger volume of OP1 in the left hemisphere than in the right hemisphere in adults (Eickhoff et al. 2006). Leftward area asymmetry in the PT and Heschl's gyrus was also consistently found at birth, 1, and 2 years of age, confirming the results in the previous studies in the neonates (Witelson and Pallie 1973) and adults (Lyttelton et al. 2009; Van Essen et al. 2011). The anterior portion of the SF, close to Broca's region, also showed leftward area asymmetry consistently at birth, 1, and 2 years of age. This asymmetry has been previously shown in a preterm newborn study (Dubois et al. 2010), and cytoarchitectonic asymmetries in Broca's regions also have been found to increase with the age during infancy and childhood beginning at 1 year of age (Amunts et al. 2003). Males consistently have larger sizes of significant clusters than females at birth, 1, and 2 years of age. Moreover, in males, the rightward area

asymmetries were mainly located in the inferior parietal cortex, cuneus cortex, and parieto-occipital sulcus, while in females the rightward area asymmetries were mainly located in the STS. These results might suggest that considerable gender effects on local surface area asymmetries arise before birth and persist from birth to 2 years of age. Rightward area asymmetry in the STS at birth, 1, and 2 years of age was consistent with the findings of a larger right STS than the left STS in the preterm newborn (Dubois et al. 2008) and children (Blanton et al. 2001). Based on the above findings, we suggest that left–right local surface area asymmetries in our study are most likely a result of the asymmetric brain growth around the peri-Sylvian region in fetuses, where the superior temporal gyrus and temporal operculum grew faster in the right hemisphere than in the left hemisphere, and the frontal operculum expanded faster in the left hemisphere than in the right hemisphere (Rajagopalan et al. 2011, 2012). These asymmetric peri-Sylvian regions have been found to play a major role in the speech perception and production in the adult brain (Dehaene-Lambertz et al. 2006). Since the cortical connectivity is thought to be the major driving force of cortical folding (Van Essen 1997; Nie, Guo, et al. 2011), white matter asymmetries might contribute to the cortical asymmetries around the peri-Sylvian region. For example, a diffusion tensor imaging study in infants has shown a larger left volume of the fibers of arcuate fasciculus in the temporal region (Dubois et al. 2009).

One limitation in this study is that there exists many different definitions of the sulcal depth (Li et al. 2009) in the literature, such as the distance to the nearest point in the cerebral hull surface (Van Essen 2005; Im et al. 2008; Lohmann et al. 2008), the geodesic distance along the cortical surface to gyral crests (Rettmann et al. 2002), the distance of the path constrained in cerebrospinal fluid regions to the cerebral hull surface (Kao et al. 2007), and the distance of the streamline with one-to-one mapping between the cortical surface and the cerebral hull surface using Laplace's equation (Jones et al. 2000). Although different definitions of sulcal depth might have influence on asymmetries in highly folded sulcal regions, in the study, the sulcal depth was defined as the distance from each vertex to the nearest point in the cerebral hull surface for a closer comparison with previous studies (Van Essen 2005; Hill et al. 2010). Another limitation is related to the statistical analysis of cortical asymmetries. When performing the statistical analysis of asymmetries using TFCE, we performed the analysis in the whole population, the male group, and the female group, respectively. Following the strategy in Hill et al. (2010), we did not remove the effects of many subject characteristics, such as brain volume and gestational age (weeks), which might have some influences on the asymmetries.

Conclusion

By using infant-specific postprocessing methods and surface-based morphometry, we have systemically and quantitatively characterized the cortical hemispheric structural asymmetries using vertex position, sulcal depth, mean curvature, and local surface area at birth, 1, and 2 years of age, via longitudinal MRI data from a cohort of 73 healthy subjects. To our knowledge, this is the first study of longitudinal developmental trajectories and sexual dimorphisms of cortical structural

asymmetries in early postnatal stages. We find that prominent cortical structural asymmetries around the peri-Sylvian region and STS are present at birth and evolve modestly from birth to 2 years of age. Preceding studies in infants only investigated cortical structural asymmetries of vertex positions at several specific regions in contrast to investigation of the asymmetries of vertex positions of all cortical regions as we did in this study. In addition, we find more clusters of sulcal depth and local surface area asymmetries than previous studies in infants. Moreover, for the first time, we find that considerable sexual dimorphisms of cortical structural asymmetries are present at birth, with males having larger magnitudes and sizes of significant clusters of cortical structural asymmetries than females that persist from birth to 2 years of age. Considering the major role of these asymmetric peri-Sylvian regions in the speech perception and production, it would be interesting to investigate how these early cortical structural asymmetries relate to the development of functional lateralization for language in infants.

Notes

Conflict of Interest: None declared.

References

Amunts K, Schleicher A, Ditterich A, Zilles K. 2003. Broca's region: cytoarchitectonic asymmetry and developmental changes. J Comp Neurol. 465:72–89.

Blanton RE, Levitt JG, Thompson PM, Narr KL, Capetillo-Cunliffe L, Nobel A, Singerman JD, McCracken JT, Toga AW. 2001. Mapping cortical asymmetry and complexity patterns in normal children. Psychiatry Res. 107:29–43.

Cachia A, Mangin JF, Riviere D, Kherif F, Boddaert N, Andrade A, Papadopoulos-Orfanos D, Poline JB, Bloch I, Zilbovicius M et al. 2003. A primal sketch of the cortex mean curvature: a morphogenesis based approach to study the variability of the folding patterns. IEEE Trans Med Imaging. 22:754–765.

Cao J, Worsley KJ. 1999. The detection of local shape changes via the geometry of Hotelling's T-2 fields. Ann Stat. 27:925–942.

Chandana SR, Behen ME, Juhasz C, Muzik O, Rothermel RD, Mangner TJ, Chakraborty PK, Chugani HT, Chugani DC. 2005. Significance of abnormalities in developmental trajectory and asymmetry of cortical serotonin synthesis in autism. Int J Dev Neurosci. 23:171–182.

Chi JG, Dooling EC. 1976. Gyral development of the human brain. Trans Am Neurol Assoc. 101:89–90.

Chi JG, Dooling EC, Gilles FH. 1977. Gyral development of the human brain. Ann Neurol. 1:86–93.

Chung MK, Worsley KJ, Nacewicz BM, Dalton KM, Davidson RJ. 2010. General multivariate linear modeling of surface shapes using Surf-Stat. Neuroimage. 53:491–505.

Davatzikos C, Bryan RN. 2002. Morphometric analysis of cortical sulci using parametric ribbons: a study of the central sulcus. J Comput Assist Tomogr. 26:298–307.

Dehaene-Lambertz G, Hertz-Pannier L, Dubois J. 2006. Nature and nurture in language acquisition: anatomical and functional brain-imaging studies in infants. Trends Neurosci. 29:367–373.

Draca S. 2010. Gender-specific functional cerebral asymmetries and unilateral cerebral lesion sequelae. Rev Neurosci. 21:421–425.

Dubois J, Benders M, Cachia A, Lazeyras F, Ha-Vinh Leuchter R, Sizonenko SV, Borradori-Tolsa C, Mangin JF, Huppi PS. 2008. Mapping the early cortical folding process in the preterm newborn brain. Cereb Cortex. 18:1444–1454.

Dubois J, Benders M, Lazeyras F, Borradori-Tolsa C, Leuchter RH, Mangin JF, Huppi PS. 2010. Structural asymmetries of perisylvian regions in the preterm newborn. Neuroimage. 52:32–42.

Dubois J, Hertz-Pannier L, Cachia A, Mangin JF, Le Bihan D, Dehaene-Lambertz G. 2009. Structural asymmetries in the infant language and sensori-motor networks. Cereb Cortex. 19:414–423.

Eickhoff SB, Amunts K, Mohlberg H, Zilles K. 2006. The human parietal operculum. II. Stereotaxic maps and correlation with functional imaging results. Cereb Cortex. 16:268–279.

Fischl B, Sereno MI, Dale AM. 1999. Cortical surface-based analysis. II: inflation, flattening, and a surface-based coordinate system. Neuroimage. 9:195–207.

Geschwind N, Galaburda AM. 1985. Cerebral lateralization. Biological mechanisms, associations, and pathology: I. A hypothesis and a program for research. Arch Neurol. 42:428–459.

Geschwind N, Levitsky W. 1968. Human brain: left-right asymmetries in temporal speech region. Science. 161:186–187.

Gilmore JH, Lin W, Prastawa MW, Looney CB, Vetsa YS, Knickmeyer RC, Evans DD, Smith JK, Hamer RM, Lieberman JA et al. 2007. Regional gray matter growth, sexual dimorphism, and cerebral asymmetry in the neonatal brain. J Neurosci. 27:1255–1260.

Gilmore JH, Shi F, Woolson SL, Knickmeyer RC, Short SJ, Lin W, Zhu H, Hamer RM, Styner M, Shen D. 2011. Longitudinal development of cortical and subcortical gray matter from birth to 2 years. Cereb Cortex. 22:2478–2485.

Glasel H, Leroy F, Dubois J, Hertz-Pannier L, Mangin JF, Dehaene-Lambertz G. 2011. A robust cerebral asymmetry in the infant brain: the rightward superior temporal sulcus. Neuroimage. 58:716–723.

Goldstein JM, Seidman LJ, O'Brien LM, Horton NJ, Kennedy DN, Makris N, Caviness VS Jr, Faraone SV, Tsuang MT. 2002. Impact of normal sexual dimorphisms on sex differences in structural brain abnormalities in schizophrenia assessed by magnetic resonance imaging. Arch Gen Psychiatry. 59:154–164.

Habas PA, Scott JA, Roosta A, Rajagopalan V, Kim K, Rousseau F, Barkovich AJ, Glenn OA, Studholme C. 2012. Early folding patterns and asymmetries of the normal human brain detected from in utero MRI. Cereb Cortex. 22:13–25.

Hamilton LS, Narr KL, Luders E, Szeszko PR, Thompson PM, Bilder RM, Toga AW. 2007. Asymmetries of cortical thickness: effects of handedness, sex, and schizophrenia. Neuroreport. 18:1427–1431.

Herbert MR, Ziegler DA, Deutsch CK, O'Brien LM, Kennedy DN, Filipek PA, Bakardjiev AI, Hodgson J, Takeoka M, Makris N Jr et al. 2005. Brain asymmetries in autism and developmental language disorder: a nested whole-brain analysis. Brain. 128:213–226.

Hill J, Dierker D, Neil J, Inder T, Knutsen A, Harwell J, Coalson T, Van Essen D. 2010. A surface-based analysis of hemispheric asymmetries and folding of cerebral cortex in term-born human infants. J Neurosci. 30:2268–2276.

Im K, Lee JM, Lyttelton O, Kim SH, Evans AC, Kim SI. 2008. Brain size and cortical structure in the adult human brain. Cereb Cortex. 18:2181–2191.

Jones SE, Buchbinder BR, Aharon I. 2000. Three-dimensional mapping of cortical thickness using Laplace's equation. Hum Brain Mapp. 11:12–32.

Kao CY, Hofer M, Sapiro G, Stem J, Rehm K, Rottenberg DA. 2007. A geometric method for automatic extraction of sulcal fundi. IEEE Trans Med Imaging. 26:530–540.

Kasprian G, Langs G, Brugger PC, Bittner M, Weber M, Arantes M, Prayer D. 2011. The prenatal origin of hemispheric asymmetry: an in utero neuroimaging study. Cereb Cortex. 21:1076–1083.

Lange N, Dubray MB, Lee JE, Froimowitz MP, Froehlich A, Adluru N, Wright B, Ravichandran C, Fletcher PT, Bigler ED et al. 2010. Atypical diffusion tensor hemispheric asymmetry in autism. Autism Res. 3:350–358.

Li G, Guo L, Nie J, Liu T. 2009. Automatic cortical sulcal parcellation based on surface principal direction flow field tracking. Neuroimage. 46:923–937.

Li G, Guo L, Nie J, Liu T. 2010. An automated pipeline for cortical sulcal fundi extraction. Med Image Anal. 14:343–359.

Li G, Nie J, Wang L, Shi F, Lin W, Gilmore JH, Shen D. 2012. Mapping region-specific longitudinal cortical surface expansion from birth to 2 years of age. Cereb Cortex. (in press).

Li G, Nie J, Wu G, Wang Y, Shen D. 2012. Consistent reconstruction of cortical surfaces from longitudinal brain MR images. Neuroimage. 59:3805–3820

Lin PY, Roche-Labarbe N, Dehaes M, Fenoglio A, Grant PE, Franceschini MA. 2012. Regional and hemispheric asymmetries of cerebral hemodynamic and oxygen metabolism in newborns. Cereb Cortex. (in press).

Lohmann G, von Cramon DY, Colchester AC. 2008. Deep sulcal landmarks provide an organizing framework for human cortical folding. Cereb Cortex. 18:1415–1420.

Luders E, Narr KL, Thompson PM, Rex DE, Jancke L, Toga AW. 2006. Hemispheric asymmetries in cortical thickness. Cereb Cortex. 16:1232–1238.

Lyttelton OC, Karama S, Ad-Dab'bagh Y, Zatorre RJ, Carbonell F, Worsley K, Evans AC. 2009. Positional and surface area asymmetry of the human cerebral cortex. Neuroimage. 46:895–903.

McGlone J. 1978. Sex differences in functional brain asymmetry. Cortex. 14:122–128.

Narr KL, Bilder RM, Luders E, Thompson PM, Woods RP, Robinson D, Szeszko PR, Dimtcheva T, Gurbani M, Toga AW. 2007. Asymmetries of cortical shape: effects of handedness, sex and schizophrenia. Neuroimage. 34:939–948.

Narr KL, Thompson PM, Sharma T, Moussai J, Blanton R, Anvar B, Edris A, Krupp R, Rayman J, Khaledy M et al. 2001. Three-dimensional mapping of temporo-limbic regions and the lateral ventricles in schizophrenia: gender effects. Biol Psychiatry. 50:84–97.

Narr KL, Thompson PM, Sharma T, Moussai J, Zoumalan C, Rayman J, Toga A. 2001. Three-dimensional mapping of gyral shape and cortical surface asymmetries in schizophrenia: gender effects. Am J Psychiatry. 158:244–255.

Nie J, Guo L, Li G, Faraco C, Stephen Miller L, Liu T. 2010. A computational model of cerebral cortex folding. J Theor Biol. 264:467–478.

Nie J, Guo L, Li K, Wang Y, Chen G, Li L, Chen H, Deng F, Jiang X, Zhang T et al. 2011. Axonal fiber terminations concentrate on gyri. Cereb Cortex. 22:2831–2839.

Nie J, Li G, Wang L, Gilmore JH, Lin W, Shen D. 2011. A computational growth model for measuring dynamic cortical development in the first year of life. Cereb Cortex. 22:2272–2284.

Ochiai T, Grimault S, Scavarda D, Roch G, Hori T, Riviere D, Mangin JF, Regis J. 2004. Sulcal pattern and morphology of the superior temporal sulcus. Neuroimage. 22:706–719.

Rajagopalan V, Scott J, Habas PA, Kim K, Corbett-Detig J, Rousseau F, Barkovich AJ, Glenn OA, Studholme C. 2011. Local tissue growth patterns underlying normal fetal human brain gyrification quantified in utero. J Neurosci. 31:2878–2887.

Rajagopalan V, Scott J, Habas PA, Kim K, Rousseau F, Glenn OA, Barkovich AJ, Studholme C. 2012. Mapping directionality specific volume changes using tensor based morphometry: an application to the study of gyrogenesis and lateralization of the human fetal brain. Neuroimage. 63:947–958

Rettmann ME, Han X, Xu C, Prince JL. 2002. Automated sulcal segmentation using watersheds on the cortical surface. Neuroimage. 15:329–344.

Shaw P, Lalonde F, Lepage C, Rabin C, Eckstrand K, Sharp W, Greenstein D, Evans A, Giedd JN, Rapoport J. 2009. Development of cortical asymmetry in typically developing children and its disruption in attention-deficit/hyperactivity disorder. Arch Gen Psychiatry. 66:888–896.

Shaywitz BA, Shaywitz SE, Pugh KR, Constable RT, Skudlarski P, Fulbright RK, Bronen RA, Fletcher JM, Shankweiler DP, Katz L et al. 1995. Sex differences in the functional organization of the brain for language. Nature. 373:607–609.

Shen D, Davatzikos C. 2004. Measuring temporal morphological changes robustly in brain MR images via 4-dimensional template warping. Neuroimage. 21:1508–1517.

Shi F, Fan Y, Tang S, Gilmore JH, Lin W, Shen D. 2010. Neonatal brain image segmentation in longitudinal MRI studies. Neuroimage. 49:391–400.

Shi F, Wang L, Dai Y, Gilmore JH, Lin W, Shen D. 2012. LABEL: pediatric brain extraction using learning-based meta-algorithm. Neuroimage. 62:1975–1986.

Shi F, Yap PT, Wu G, Jia H, Gilmore JH, Lin W, Shen D. 2011. Infant brain atlases from neonates to 1- and 2-year-olds. PLoS One. 6: e18746.

Sled JG, Zijdenbos AP, Evans AC. 1998. A nonparametric method for automatic correction of intensity nonuniformity in MRI data. IEEE Trans Med Imaging. 17:87–97.

Smith SM, Nichols TE. 2009. Threshold-free cluster enhancement: addressing problems of smoothing, threshold dependence and localisation in cluster inference. Neuroimage. 44:83–98.

Sommer I, Ramsey N, Kahn R, Aleman A, Bouma A. 2001. Handedness, language lateralisation and anatomical asymmetry in schizophrenia: meta-analysis. Br J Psychiatry. 178:344–351.

Sowell ER, Thompson PM, Peterson BS, Mattson SN, Welcome SE, Henkenius AL, Riley EP, Jernigan TL, Toga AW. 2002. Mapping cortical gray matter asymmetry patterns in adolescents with heavy prenatal alcohol exposure. Neuroimage. 17:1807–1819.

Sowell ER, Thompson PM, Rex D, Kornsand D, Tessner KD, Jernigan TL, Toga AW. 2002. Mapping sulcal pattern asymmetry and local cortical surface gray matter distribution in vivo: maturation in perisylvian cortices. Cereb Cortex. 12:17–26.

Sun T, Patoine C, Abu-Khalil A, Visvader J, Sum E, Cherry TJ, Orkin SH, Geschwind DH, Walsh CA. 2005. Early asymmetry of gene transcription in embryonic human left and right cerebral cortex. Science. 308:1794–1798.

Sun T, Walsh CA. 2006. Molecular approaches to brain asymmetry and handedness. Nat Rev Neurosci. 7:655–662.

Thompson PM, Moussai J, Zohoori S, Goldkorn A, Khan AA, Mega MS, Small GW, Cummings JL, Toga AW. 1998. Cortical variability and asymmetry in normal aging and Alzheimer's disease. Cereb Cortex. 8:492–509.

Toga AW, Thompson PM. 2003. Mapping brain asymmetry. Nat Rev Neurosci. 4:37–48.

Van Essen DC. 2005. A population-average, landmark- and surface-based (PALS) atlas of human cerebral cortex. Neuroimage. 28:635–662.

Van Essen DC. 1997. A tension-based theory of morphogenesis and compact wiring in the central nervous system. Nature. 385:313–318.

Van Essen DC, Dierker DL. 2007. Surface-based and probabilistic atlases of primate cerebral cortex. Neuron. 56:209–225.

Van Essen DC, Glasser MF, Dierker DL, Harwell J, Coalson T. 2011. Parcellations and hemispheric asymmetries of human cerebral cortex analyzed on surface-based atlases. Cereb Cortex. 22:2241–2262

Wada JA, Clarke R, Hamm A. 1975. Cerebral hemispheric asymmetry in humans. Cortical speech zones in 100 adults and 100 infant brains. Arch Neurol. 32:239–246.

Wang L, Shi F, Yap PT, Lin W, Gilmore JH, Shen D. 2011. Longitudinally guided tissue segmentation of neonates. Hum Brain Mapp. (in press).

Watkins KE, Paus T, Lerch JP, Zijdenbos A, Collins DL, Neelin P, Taylor J, Worsley KJ, Evans AC. 2001. Structural asymmetries in the human brain: a voxel-based statistical analysis of 142 MRI scans. Cereb Cortex. 11:868–877.

Witelson SF, Pallie W. 1973. Left hemisphere specialization for language in the newborn. Neuroanatomical evidence of asymmetry. Brain. 96:641–646.

Worsley KJ, Taylor JE, Tomaiuolo F, Lerch J. 2004. Unified univariate and multivariate random field theory. Neuroimage. 23(Suppl 1): S189–S195.

Wu G, Qi F, Shen D. 2006. Learning-based deformable registration of MR brain images. IEEE Trans Med Imaging. 25:1145–1157.

Xue Z, Shen D, Davatzikos C. 2006. CLASSIC: consistent longitudinal alignment and segmentation for serial image computing. Neuroimage. 30:388–399.

Yeo BT, Sabuncu MR, Vercauteren T, Ayache N, Fischl B, Golland P. 2010. Spherical demons: fast diffeomorphic landmark-free surface registration. IEEE Trans Med Imaging. 29:650–668.